





Imaging of combined hepatocellular-cholangiocarcinoma in cirrhosis and risk of false diagnosis of hepatocellular carcinoma

Elisabetta Sagrini¹, Massimo Iavarone², Federico Stefanini¹,
Francesco Tovoli¹ , Sara Vavassori², Marco Maggioni², Matteo Renzulli³,
Veronica Salvatore¹, Horia Stefanescu¹, Massimo Colombo², Luigi Bolondi¹
and Fabio Piscaglia¹ 

Abstract

Background: Diagnosis of hepatocellular carcinoma can be achieved by imaging in cirrhotic patients. Combined hepatocellular-cholangiocarcinoma is a primary liver tumor and its imaging patterns have been poorly investigated. Misdiagnosis for either hepatocellular carcinoma or benign lesions can occur. We aimed to evaluate the enhancement pattern of combined hepatocellular-cholangiocarcinoma in cirrhosis with imaging techniques and to estimate the risk of misdiagnosis for hepatocellular carcinoma.

Methods: All histology-confirmed combined hepatocellular-cholangiocarcinoma in cirrhosis seen in two Italian centers between 2003 and 2016, in which at least one imaging technique had been performed, was retrospectively collected. The enhancement pattern was analyzed for all available imaging modalities.

Results: A total of 37 combined hepatocellular-cholangiocarcinoma nodules were identified. Contrast-enhanced ultrasound, computed tomography, and magnetic resonance imaging had been performed in 27, 34, and 17 nodules, respectively. Contrast-enhanced ultrasound was at higher risk of misdiagnosis for pure hepatocellular carcinoma than computed tomography ($p=0.005$) or magnetic resonance imaging ($p=0.040$). Only six of 24 combined hepatocellular-cholangiocarcinoma lesions submitted to both contrast-enhanced ultrasound and computed tomography showed coincident patterns; contrast-enhanced ultrasound correctly suggested a condition of malignancy in a higher number of cases than computed tomography ($p<0.001$) and magnetic resonance imaging ($p=0.002$).

Conclusions: Contrast-enhanced ultrasound misdiagnosed a higher number of combined hepatocellular-cholangiocarcinoma as hepatocellular carcinoma than computed tomography and magnetic resonance imaging. However, the latter techniques were able to identify features of malignancy less often.

Keywords

Liver tumors, primary liver cancer, contrast-enhanced ultrasound, CEUS, liver imaging

Received: 25 August 2018; accepted: 13 October 2018

Key summary

What did we already know?

1. Diagnosis of hepatocellular carcinoma can be achieved by imaging in cirrhotic patients.
2. Combined hepatocellular-cholangiocarcinoma may be a cause of misdiagnosis at imaging.

¹Department of Medical and Surgical Sciences, University of Bologna, Bologna, Italy

²First Division of Gastroenterology, University of Milan, Milan, Italy

³Radiology Unit, S. Orsola-Malpighi Bologna Authority Hospital, Bologna, Italy

Corresponding author:

Francesco Tovoli, Department of Medical and Surgical Sciences, University of Bologna, Via Albertoni 15, 40138, Bologna, Italy.
Email: francesco.tovoli2@unibo.it

3. The imaging pattern of combined hepatocellular-cholangiocarcinoma in liver cirrhosis has been poorly investigated.

What are the significant findings of this study?

1. Imaging characteristics of combined hepatocellular-cholangiocarcinoma in cirrhosis are heterogeneous.
2. Contrast-enhanced ultrasound better identified features of malignancy compared to computed tomography and magnetic resonance imaging.
3. However, computed tomography and magnetic resonance imaging misdiagnosed a lower number of combined hepatocellular-cholangiocarcinomas as hepatocellular carcinomas compared to contrast-enhanced ultrasound.
4. Discrepant results between the imaging techniques should prompt further investigation to avoid misclassification of combined hepatocellular-cholangiocarcinoma as a pure hepatocellular carcinoma.

Introduction

Combined hepatocellular–cholangiocellular carcinoma (CHC) is a primary liver cancer composed of a combination of cholangiocyte- and hepatocyte-derived malignant cells coexisting in the same tumor.^{1–4} This tumor may arise from a common bipotential hepatic progenitor cell in a continuum between intrahepatic cholangiocarcinoma (ICC), CHC and hepatocellular carcinoma (HCC).^{5–9}

Cirrhotic patients undergo semiannual ultrasound surveillance for early detection of de-novo nodules because they are at higher risk of developing primary liver malignancies. Non-invasive diagnostic criteria for HCC have been validated and incorporated in the international guidelines.^{5,10,11} A precise differentiation between HCC and other less-frequent primary malignant focal lesions is of great importance to properly establish a treatment strategy. In fact, the efficacy of treatments such as transplantation or sorafenib has not been demonstrated in CHC or ICC.^{12,13}

Some data showed a risk of misdiagnosis between ICC and HCC in cirrhotic patients when investigated with contrast-enhanced ultrasound (CEUS).^{14–16} Accordingly, CEUS was dropped from the American Association for the Study of Liver Disease guidelines as a diagnostic imaging method. Imaging patterns of ICC and HCC differ one from another.^{5,11,14,17} The American College of Radiology (ACR) Liver Imaging Reporting and Data System (LI-RADS) was recently developed to standardize, interpret, report, and collect data for CEUS, computed tomography (CT), and magnetic resonance imaging (MRI) in patients at risk for developing HCC.^{18,19} No specific data exist on the imaging features of CHC in cirrhotic patients and the rate of patients with CHC at risk of misclassification for HCC. Existing studies consist of limited populations, largely composed of patients without chronic viral hepatitis or cirrhosis, for which imaging diagnosis of HCC is not accepted.^{20–23}

Therefore, the primary aim of the study was to evaluate the imaging features of CHC in cirrhosis with CEUS, CT, and MRI. The secondary aim was to evaluate the rate of CHC showing typical features for HCC, thus the rate of CHC at risk of misdiagnosis with HCC.

Patients and methods

Study population

We retrospectively searched for all consecutive patients with cirrhosis and histology-confirmed CHC, evaluated in two Italian referral centers between 2003 and 2016. The date of 2003 was set to identify patients investigated with modern contrast imaging techniques including real-time CEUS. The following addition inclusion criteria were used: (a) high risk of developing HCC, according to international guidelines,^{5,11,24} (b) availability of at least one contrast imaging technique (CEUS, CT or MRI) performed on the nodule subjected to histology, and (c) type B or C CHC according to Allen-Lisa classification.¹ Cirrhosis was diagnosed by histology, when available, or by a combination of clinical, laboratory, and ultrasonographic features.

The name and date of approval granted by the Ethical Board are included in the Ethics section of the manuscript.

Imaging techniques

CEUS examinations were performed using the convex probe at low mechanical index ($MI < 0.1$). A bolus injection of sulfur hexafluoride (Sonovue, Bracco, Milan, Italy) was utilized as the contrast agent in both centers, at a dosage of 1.5–2.4 mL, depending on the different types of equipment as repeatedly reported by both centers.²⁵ All CEUS studies were performed at the two study centers.

The lesion enhancement pattern was studied in three temporal phases: arterial (10–30 s after injection), portal (30–120 s), and late phase (>120 s), according to European Federation of Societies for Ultrasound in Medicine and Biology recommendations.^{10,26}

Contrast-enhanced CT and MRI scans were performed according to each institution's protocol for focal liver lesions in cirrhotic patients. Given the retrospective nature of the study, some imaging exams were performed outside the study institutions. Such studies were included if image quality was adequate. Enhancement patterns were ascribed to two main vascular phases: arterial and venous/delayed phases, using iodine and/or gadolinium contrast agent. Venous and delayed phases were incorporated in one single category, considering the least enhancement aspect to verify the occurrence of wash-out. All available information was re-evaluated by a radiologist in consensus with clinicians with extensive experience in contrast ultrasonography of the liver.

The tumor contrast vascular patterns were classified as follows:

- Homogeneous hyper-enhancement (global contrast enhancement grossly more than 75% of the whole tumor, Figure 1).
- Heterogeneous hyper-enhancement (irregular contrast enhancement but estimated grossly more than 25% of the tumor).
- Rim-like hyper-enhancement (peripheral hyper-enhancement of the lesion with an extension no

greater than 25% of the whole tumor surrounding a central area of relative hypo-enhancement, Figure 2).

- Global iso-enhancement (same enhancement as the surrounding liver parenchyma).
- Global hypo-enhancement (less enhancement than the surrounding liver parenchyma).

Wash-out of the contrast media was recorded if the lesion became hypo-enhanced in the portal or late phase following a hyper-enhanced or iso-enhanced appearance during the arterial phase, irrespective of the pattern of hyper-enhancement.

Classical definition of malignant nodules and typical HCC. For the purpose of our study, the reliability of imaging methods was assessed by evaluating: (a) their accuracy in suggesting a malignant nature of the nodule; and (b) the rate of nodules not showing a typical pattern for HCC in cirrhosis, thus correctly prompting further workup to reach a final diagnosis.

A nodule was considered malignant if it showed arterial phase enhancement followed by wash-out in any phase. A nodule was defined as typical HCC if it showed arterial enhancement followed by a late (>60 s) and mild wash-out.

ACR LI-RADS classification. The ACR supports both CEUS LI-RADS¹⁸ and CT/MRI LI-RADS¹⁹ classification systems.

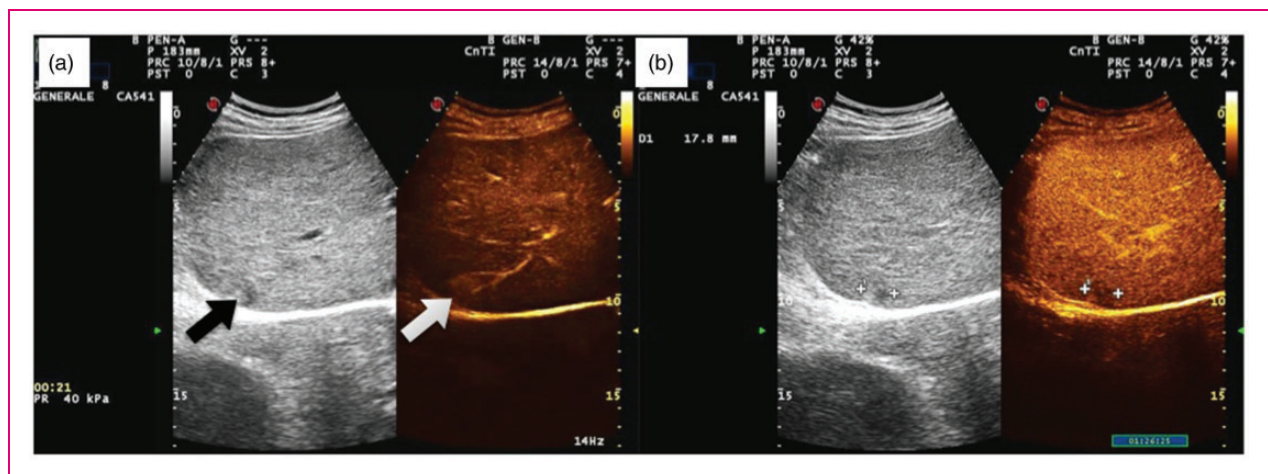


Figure 1. Contrast-enhanced appearance of a combined hepatocellular–cholangiocellular carcinoma (CHC) nodule at risk of misdiagnosis with typical hepatocellular carcinoma (HCC) on dual imaging with real-time contrast-enhanced ultrasound (CEUS) examination. (a) On the left, inhomogeneous subcapsular nodule in cirrhosis on B-mode ultrasound (black arrow). Subcapsular CHC in cirrhosis displaying a homogeneous arterial hyper-enhancement in CEUS (white arrow). (b) Wash-out of the nodule in the portal phase (1 min 26 sec post-injection).

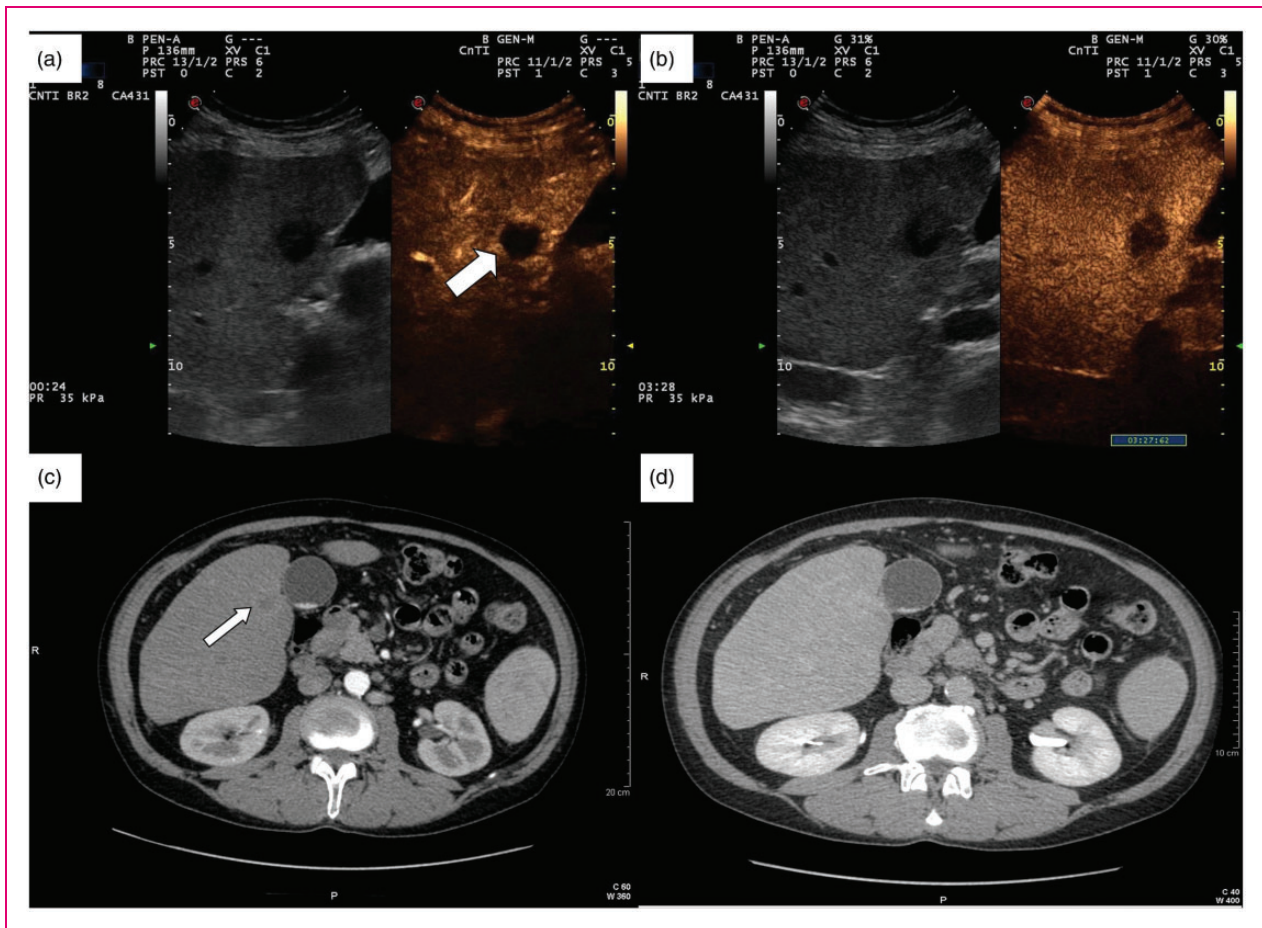


Figure 2. (a) Contrast-enhanced ultrasound (CEUS) rim-like appearance of a combined hepatocellular–cholangiocellular carcinoma (CHC) nodule during the arterial phase (white thick arrow). (b) The enhancement of the rim fades out in late phase (3 min 26 sec post-injection), with a persistently hypoechoic central area. (c) Contrast-enhanced computed tomography (CT) of the same CHC nodule shows a mild arterial rim-like enhancement (thin arrow). (d) The enhancement progresses towards being mild homogeneous centripetal during the portal-late phase.

Briefly, CEUS LI-RADS estimate the risk of malignancy based on the following factors: presence or absence of arterial phase enhancement, size, presence or absence of wash-out of any type, late and mild wash-out pattern. Based on these characteristics, a nodule can be classified as LR-3 (intermediate malignancy probability), LR-4 (probable HCC), or LR-5 (definite HCC). Notably, a nodule is classified as LR-M (definitely malignant but not HCC-specific) if any of the following characteristics are found: rim-like arterial hyper-enhancement, early wash-out (<60 s), or marked wash-out.

The CT/MRI LI-RADS system is similar. Nodules are classified according to arterial peripheral enhancement, size, wash-out, enhancing capsule, and threshold growth. Again, patients with rim-like arterial enhancement are classified as LR-M.

Ethics. The protocol was approved by the Ethics Committee (n°78/2017/O/OssN, 27/03/2017) and

conformed to the guidelines of the 1975 Declaration of Helsinki. Informed consent was waived given the retrospective nature of the study.

Statistical analysis. Continuous variables were expressed as median and range. Categorical variables were expressed as count and percentage. Differences in the imaging patterns were performed applying chi-square test with Fisher exact test ($p < 0.05$ was considered significant). Statistical analyses were performed with SPSS software (SPSS statistics, IBM corporation 1989–2011, 20.0 edition).

Results

Patients characteristics

This study included 35 patients. One nodule per patient was evaluated. In two patients a recurrent CHC nodule

arose after a curative treatment. These two additional nodules were also included in the study, for a total of 37 CHC nodules.

Overall, 20 patients had a single nodule, whereas 15 patients had multifocal liver disease. Among these 15 patients, seven underwent surgical treatment. Three of them received a histological diagnosis of synchronous separate nodules of HCC and CHC.

Six patients had a recurrent nodule after the first CHC and were re-treated (radiofrequency ablation in four and resection in two patients).

The pathological diagnosis of CHC nodules was obtained by percutaneous US-guided biopsy in 20 cases, and liver resection specimen in 17 cases. Classification according to Allen-Lisa was as follows: 36 type C and one type B CHC. Clinical and laboratory data at the time of diagnosis are reported in Table 1.

Imaging findings. CEUS, CT, and MRI were performed in 27, 34, and 17 nodules, respectively.

Median nodule size was 25 mm (range 10–100). Nodule size was ≤ 2 cm in 15 cases, 2–3 cm in nine cases and > 3 cm in 13 cases.

Table 1. Demographic and clinical data of the study population. Continuous variables are expressed as median (range).

Age (years)	62 (40–77)
Male gender (%)	28 (80)
Etiology, <i>n</i> (%)	
– HBV*	8 (22.9)
– HCV**	16 (45.7)
– Alcohol	7 (20.0)
– NASH/cryptogenic	4 (11.4)
Laboratory tests	
– AST (U/L)	47.5 (11–268)
– ALT (U/L)	37 (7–217)
– Total bilirubin (mg/dl)	0.7 (0.4–27.7)
– Albumin (g/L)	41 (22–49)
– AFP (ng/ml)	10.35 (2–250)
– CA 19-9 (U/L)	41.5 (1–4920)
Tumor characteristics	
– Nodule size (mm)	25 (10–100)
– Within Milan Criteria (%)	21 (60)
– Macrovascular invasion/ extrahepatic spread (%)	7 (20)

*Three patients had an HBV/HCV co-infection; **two patients had a concurrent alcohol abuse.

HBV: hepatitis B virus; HCV: hepatitis C virus; NASH: non-alcoholic steatohepatitis; AST: aspartate aminotransferase; ALT: alanine aminotransferase; AFP: alfa-fetoprotein.

Arterial phase

Homogeneous hyper-enhancement was more frequent in CEUS (55%) compared to CT (23%) or MRI (47%). A rim-like hyper-enhancement pattern was observed more often in CT (50%) than in CEUS (26%) and MRI (29%). Heterogeneous hyper-enhancement was never reported by CEUS, but appeared in 15% and 6% of cases at CT and MRI, respectively (Table 2).

Analysis of contrast patterns according to the nodule size showed that 29% (4/14) and 22% (2/9) of CHC nodules ≤ 2 cm demonstrated the rim-like enhancement in the arterial phase at CT and MRI, respectively. No case of rim-like enhancement was observed in lesions ≤ 2 cm at CEUS. Conversely, 17/20 (85%) of CHC nodules > 2 cm in size showed rim-like or heterogeneous hyper-enhancement at the CT scan, whereas 44% (7/16) and 50% (4/8) of CHC > 2 cm showed rim-like or heterogeneous pattern in CEUS and MRI, respectively.

A small number of CHC (4/27, 15%) showed poor enhancement in the CEUS, whereas CT and MRI did not describe any hypovascular tumors.

Venous/delayed phase

During the venous phases hypo-enhancement occurred in 89% (24/27), 24% (8/34), and 30% (5/17) of CHC nodules in CEUS, CT, and MRI, respectively. The rates of iso-enhancement were 11% (3/27), 41% (14/34), and 35% (6/17), respectively.

CT showed global, peripheral, and heterogeneous hyper-enhancement in 3% (1/34), 23% (8/34), and 9% (3/34) of CHC nodules in the venous phases. MRI detected homogeneous and peripheral hyper-enhancement in 18% (3/17) and 12% (2/17) of cases whereas CEUS did not demonstrate any hyper-enhanced nodules.

Pattern of malignancy

CEUS correctly identified 78% (21/27) of CHC nodules as malignant (Table 3).

Sensitivity for malignancy increased with nodule size. A malignant pattern was shown in 7/11 (64%) nodules ≤ 2 cm, 14/16 (88%) nodules > 2 cm, 12/12 (100%) > 2.5 cm, and in 8/8 (100%) nodules > 3 cm.

CT detected a malignant pattern in a significantly lower percentage of CHC nodules (24%, 7/34) than CEUS ($p < 0.001$). Sensitivity for malignancy decreased with increasing size. A malignant pattern was observed in 2/20 (10%) and 1/16 (6%) nodules > 2 cm and > 2.5 cm, compared with 6/14 (43%) and 7/18 (39%) below these thresholds ($p = 0.035$ and $p = 0.030$, respectively).

Table 2. Analysis of the enhancement patterns in the arterial and venous/delayed phase according to the different imaging techniques.

	Arterial phase			Venous/delayed phase			Hepatobiliary phase*
	CEUS (n = 27)	CT (n = 34)	MRI (n = 17)	CEUS (n = 27)	CT (n = 34)	MRI (n = 17)	MRI (n = 17)
No hyper-enhancement (overall) (%)	5 (19)	4 (12)	3 (18)	27 (100)	22 (65)	11 (65)	15 (88)
– Hypo-enhanced (%)	1 (4)	0	0	24 (89)	8 (24)	5 (30)	
– Iso-enhanced (%)	4 (15)	4 (12)	3 (18)	3 (11)	14 (41)	6 (35)	
Hyper-enhancement (overall) (%)	22 (81)	30 (88)	14 (82)	0	12 (35)	6 (35)	2 (12)
– Homogeneously hyper-enhanced (%)	15 (55)	8 (23)	8 (47)	0	1 (3)	3 (18)	
– Peripherally rim-like hyper-enhanced (%)	7 (26)	17 (50)	5 (29)	0	8 (23)	2 (12)	
– Heterogeneously hyper-enhanced (%)	0	5 (15)	1 (6)	0	3 (9)	1 (5)	

*Hepatobiliary phase appearance at MRI is reported in the table but not analyzed in the text as not part of the European Association for the Study of the Liver and American Association for the Study of Liver Diseases guidelines for the non-invasive diagnosis of HCC in cirrhosis.

CEUS: contrast-enhanced ultrasound; CT: computed tomography; HCC: hepatocellular carcinoma; MRI: magnetic resonance imaging.

Table 3. Rate of CHC nodules characterized as malignant and at risk for misdiagnosis for HCC according to the different contrast enhanced techniques.

	CEUS (n = 27)	CT (n = 34)	MRI (n = 17)	p values
CHC nodules characterized as malignant (classical definition) (%)	21 (78%)	7 (24%)	5 (29%)	*p < 0.001, **p = 0.004, ***p = ns
CHC nodules at risk for misdiagnosis for HCC (classical definition) (%)	13 (48%)	5 (15%)	3 (18%)	*p = 0.001, **p = 0.057, ***p = ns
CHC nodules characterized as malignant (classified as LI-RADS LR-5 or LR-M) (%)	21 (78%)	22 (65%)	9 (53%)	*p = ns, **p = ns, ***p = ns
CHC nodules at risk for misdiagnosis for HCC (classified as LI-RADS LR-5) (%)	14 (52%)	4 (11%)	3 (18%)	*p = 0.001, **p = 0.030, ***p = ns

*CEUS vs CT; **CEUS vs MRI; ***CT versus MRI.

CEUS: contrast-enhanced ultrasound; CHC: combined hepatocellular-cholangiocellular carcinoma; CT: computed tomography; HCC: hepatocellular carcinoma; MRI: magnetic resonance imaging; LI-RADS: Liver Imaging Reporting and Data System.

MRI detected wash-out in 5/17 (29%) cases, a significantly lower rate than CEUS ($p = 0.002$), with no size effect on the reliability of the imaging.

CHC at risk of misdiagnosis with HCC

For pure HCC, CEUS misdiagnosed a relatively higher percentage of CHC (48%, 13/27) compared to CT (15%, 5/34; $p = 0.001$) or MRI (18%, 3/17; $p = 0.057$) (Table 3). Early or marked wash-out was found in 5/19 (26%) of nodules that were otherwise typical for HCC according to the occurrence of any hyper-enhancement in the arterial phase followed by wash-out.

CT showed a typical HCC pattern in a higher (although not statistically different), number of CHC ≤ 2 cm, respectively 4/14 (29%) versus 1/20

(5%, $p = ns$). MRI showed a pattern typical for HCC in 3/17 CHC nodules, with all of them ≤ 2 cm.

LI-RADS classification

Amongst the 27 CHC nodules evaluated with CEUS, five were classified as LR-3 (18.5%), one as LR-4 (3.7%), 14 as LR-5 (51.9%; typical HCC), and seven as LR-M (25.9%, malignant but not typical for HCC). The classification of the 34 CHC nodules evaluated with CT was as follows: LR-3 (three nodules, 8.8%), LR-4 (nine nodules, 26.5%), LR-5 (four nodules, 11.8%), and LR-M (18 nodules, 52.9%). In total, 17 nodular lesions were evaluated with MRI. Amongst them, two nodules were classified as LR-3 (11.8%), six nodules as LR-4 (35.3%), three nodules as LR-5

(17.6%), and six nodules as LR-M (35.3%). Using the LI-RADS classifications, the ability of CEUS in discriminating the malignant nature of the nodules (LR-5 + LR-M vs LR-4 + LR-3) was not significantly different from that of CT or MRI ($p=0.397$ and $p=0.105$, respectively). Instead, CEUS had a superior risk of misdiagnosis of HCC compared to CT ($p=0.001$) and MRI ($p=0.030$).

Concordance at multimodality imaging assessment (CEUS, CT, MRI)

Only six of 24 CHC lesions submitted to both CEUS and CT showed coincident enhancement patterns (four positive for wash-out and two negative). CEUS suggested a condition of malignancy in a higher number of cases (19/24, 79%) than CT (7/24, 29%), ($p=0.001$), whereas CEUS showed a pattern at risk for misdiagnosis for HCC in a higher number of CHC nodules (8/24, 33%) than CT (5/24, 21%), ($p=0.018$).

In total, 12 CHC nodules were submitted to all three imaging techniques, of which 7/12 showed an arterial hyper-enhancement pattern, three showed coincident arterial patterns (two homogeneously hyper-enhanced and one iso-enhanced), two showed a different pattern for each method and the remaining three coinciding in two methods. No nodule showed the same pattern at all three imaging techniques in the late phase. Three nodules showed a completely different vascular pattern at the three imaging techniques. In the remaining nine nodules, the coincidence was seen for two of three methods, namely in 3/12 nodules in CT/MRI, 3/12 in CT/CEUS and 3/12 CHC nodules in RM/CEUS.

Discussion

To the best of our knowledge, this is the first study focused on the imaging of CHC nodules in cirrhotic patients. We confirmed that CHC shares imaging features with both HCC and ICC.^{10,22}

Rim-like arterial enhancement (deemed atypical for HCC) was found in 26%, 50%, and 29% nodules in CEUS, CT, and MRI, respectively. This pattern has been reported with variable frequency in ICC series,²⁶ depending on the imaging method, presence of underlying cirrhosis, and size of the lesions. Its reported rates are up to 51% for CEUS and 59–65% for CT/MRI in unselected patients, whereas lower rates have been reported in cirrhosis (8–52% for CEUS)^{14,15,26} and 50% for CT.^{17,20}

Moreover, early or marked wash-out (non-typical for HCC) was found in 11/19 (58%) nodules that showed hyper-enhancement in the arterial phase followed by wash-out, highlighting the need to evaluate the characteristics of wash-out and not just its occurrence.

The enhancement pattern of lesions has also been found to be related to their size, which might also justify the different patterns in cirrhosis in which most CHC nodules could be detected when still small, thanks to the surveillance programs (different from CHC in otherwise healthy livers). Previous studies reported that most small ICCs and HCCs were homogeneously enhanced in the arterial phase, differently from those >3 cm, which are likely to show heterogeneous or peripheral enhancement.¹⁷ Similar patterns were found also in our study. This behavior is most likely related to the development of desmoplastic reaction, occurring more with the size increase, similar to what has been reported for pure ICC.^{9,27,28}

Very few CHC lesions showed coincident enhancement patterns, with the discrepancy most frequently observed in the venous phase. Those behaviors are in agreement with previous studies on ICC, in which enhancement discrepancy between delayed-phase CEUS (hypoechoogenicity) and CT (hyper or isodensity) was a common semiological finding.^{29–30} This discrepancy has been related to the different contrast agents' kinetics. SonoVue (CEUS) is a pure intravascular contrast medium that merely reflects the vascularization of the tumor, whereas iodine and gadolinium-based (CT and MRI) contrast media diffuse into the interstitium and are retained for a longer time in tissues with a desmoplastic reaction,³¹ with a large amount of fibrous stroma more frequently observed in ICC than in HCC.

These discrepancies made CT and MRI more accurate than CEUS in showing features deemed atypical for HCC in CHC nodules. However, in the case of lesions <2 cm, CT and MRI were also at a significant risk of misdiagnosis of CHC for HCC.

The iso-hyperdense pattern observed at CT or MRI during the delayed phase is a feature that CHC shares with ICC in both cirrhotic¹⁷ and non-cirrhotic livers³² and limits the risk of misclassification of ICC for HCC in cirrhosis.¹⁴ In contrast, the absence of wash-out at CT or MRI may falsely suggest a non-malignant nature, a notorious pitfall of ICC, especially for less experienced radiologists. In this study, the retrospective re-classification of the nodules according to the LI-RADS systems reduced this risk. In fact, the CT/MRI LI-RADS system acknowledges this possible pitfall and classifies all the lesions with rim-like arterial enhancement as LR-M, regardless of their pattern in the delayed phase.

Differences in enhancement patterns should not only be regarded as a limitation; they might be advantageous especially when the discrepancy patterns exist in wash-out detected by CEUS, but are absent at CT or MRI. Such a pattern is almost never observed in HCC.^{15,17,33} Nonetheless, it suggests malignancy based on the CEUS appearance, thus pointing out cholangiocellular

components of malignancy. Such consideration highlights the benefit of using more than one contrast technique in nodules not eligible for biopsy to avoid false-negative findings of malignancy (which are rare in CEUS).

These findings confirm that non-invasive diagnosis of small nodules in cirrhosis can be challenging. Whenever a doubt about a nodule in cirrhosis arises because of the lack of typical diagnostic features or discrepancy among imaging techniques, biopsy remains warranted.

The limitations of this study include its retrospective nature, its limited sample size, and the absence of a control group of HCC or ICC for comparison. However, such limitations are difficult to overcome because CHC is rare, thus a retrospective search of cases and systematic biopsy of all lesions is not possible given the chance of noninvasive diagnosis of HCC at present. Despite these limitations, it is important to highlight that our patient population is the largest that deals with cirrhotic patients. Given the retrospective and multicentric nature of this study, the available imaging records were heterogeneous but it is hard to find many cases deriving from a single center of such a rare tumor, making a prospective study nearly impossible.

In conclusion, CHC shares some imaging features with ICC such as a rim-like arterial enhancement pattern, early or marked wash-out, and the discrepancy between the CEUS and CT/MRI appearance in the late phases. Although the LI-RADS system seems to favor a more accurate classification, a combination of different imaging techniques remains of potential benefit, especially in cases not amenable to biopsy.

Acknowledgments

None to declare.

Declaration of conflicting interests

The authors have no conflicts of interest to declare.

Funding

This research received no specific grant from any funding agency in the public, commercial, or not-for-profit sectors.

Informed consent


Informed consent was waived given the retrospective nature of the study.

Ethics approval

The protocol was approved by the Ethics Committee (n°78/2017/O/OssN, 27/03/2017) and conformed to the guidelines of the 1975 Declaration of Helsinki.

ORCID iD

Francesco Tovoli  <http://orcid.org/0000-0002-8350-1155>

Fabio Piscaglia  <http://orcid.org/0000-0001-8264-1845>

References

- Allen RA and Lisa JR. Combined liver cell and bile duct carcinoma. *Am J Pathol* 1949; 25: 647–655.
- Goodman ZD, Ishak KG, Langloss JM, et al. Combined hepatocellular-cholangiocarcinoma. A histologic and immunohistochemical study. *Cancer* 1985; 55: 124–135.
- Maeda T, Adachi E, Kajiyama K, et al. Combined hepatocellular and cholangiocarcinoma: Proposed criteria according to cytokeratin expression and analysis of clinicopathologic features. *Hum Pathol* 1995; 26: 956–964.
- Yano Y, Yamamoto J, Kosuge T, et al. Combined hepatocellular and cholangiocarcinoma: A clinicopathologic study of 26 resected cases. *Jpn J Clin Oncol* 2003; 33: 283–287.
- Bruix J and Sherman M. Management of hepatocellular carcinoma: An update. *Hepatology* 2011; 53: 1020–1022.
- Komuta M, Govaere O, Vandecaveye V, et al. Histological diversity in cholangiocellular carcinoma reflects the different cholangiocyte phenotypes. *Hepatology* 2012; 55: 1876–1888.
- Coulouarn C, Cavard C, Rubbia-Brandt L, et al. Combined hepatocellular-cholangiocarcinomas exhibit progenitor features and activation of Wnt and TGFbeta signaling pathways. *Carcinogenesis* 2012; 33: 1791–1796.
- Xu J, Sasaki M, Harada K, et al. Intrahepatic cholangiocarcinoma arising in chronic advanced liver disease and the cholangiocarcinomatous component of hepatocellular cholangiocarcinoma share common phenotypes and cholangiocarcinogenesis. *Histopathology* 2011; 59: 1090–1099.
- Bridgewater J, Galle PR, Khan SA, et al. Guidelines for the diagnosis and management of intrahepatic cholangiocarcinoma. *J Hepatol* 2014; 60: 1268–1289.
- Claudon M, Dietrich CF, Choi BI, et al. Guidelines and good clinical practice recommendations for contrast enhanced ultrasound (CEUS) in the liver – update 2012: A WFUMB-EFSUMB initiative in cooperation with representatives of AFSUMB, AIUM, ASUM, FLAUS and ICUS. *Ultraschall Med* 2013; 34: 11–29.
- EASL-EORTC. clinical practice guidelines: Management of hepatocellular carcinoma. *J Hepatol* 2012; 56: 908–943.
- Wang J, Wang F and Kessinger A. Outcome of combined hepatocellular and cholangiocarcinoma of the liver. *J Oncol* 2010; 2010: 7. <https://doi.org/10.1155/2010/917356>.
- Facciuto ME, Singh MK, Lubezky N, et al. Tumors with intrahepatic bile duct differentiation in cirrhosis: Implications on outcomes after liver transplantation. *Transplantation* 2015; 99: 151–157.
- Vilana R, Forner A, Bianchi L, et al. Intrahepatic peripheral cholangiocarcinoma in cirrhosis patients may display a vascular pattern similar to hepatocellular carcinoma on contrast-enhanced ultrasound. *Hepatology* 2010; 51: 2020–2029.

15. Galassi M, Iavarone M, Rossi S, et al. Patterns of appearance and risk of misdiagnosis of intrahepatic cholangiocarcinoma in cirrhosis at contrast enhanced ultrasound. *Liver Int* 2013; 33: 771–779.
16. Li R, Zhang X, Ma KS, et al. Dynamic enhancing vascular pattern of intrahepatic peripheral cholangiocarcinoma on contrast-enhanced ultrasound: the influence of chronic hepatitis and cirrhosis. *Abdom Imaging* 2013; 38: 112–119.
17. Iavarone M, Piscaglia F, Vavassori S, et al. Contrast enhanced CT-scan to diagnose intrahepatic cholangiocarcinoma in patients with cirrhosis. *J Hepatol* 2013; 58: 1188–1193.
18. Kono Y, Lyshchik A, Cosgrove D, et al. Contrast Enhanced Ultrasound (CEUS) Liver Imaging Reporting and Data System (LI-RADS®): The official version by the American College of Radiology (ACR). *Ultraschall Med* 2017; 38: 85–86.
19. Elsayes KM, Hooker JC, Agrons MM, et al. 2017 Version of LI-RADS for CT and MR imaging: An update. *Radiographics* 2017; 37: 1994–2017.
20. Fowler KJ, Sheybani A, Parker RA, et al. Combined hepatocellular and cholangiocarcinoma (biphenotypic) tumors: Imaging features and diagnostic accuracy of contrast-enhanced CT and MRI. *AJR Am J Roentgenol* 2013; 201: 332–339.
21. de Campos RO, Semelka RC, Azevedo RM, et al. Combined hepatocellular carcinoma-cholangiocarcinoma: Report of MR appearance in eleven patients. *J Magn Reson Imaging* 2012; 36: 1139–1147.
22. Ebied O, Federle MP, Blachar A, et al. Hepatocellular-cholangiocarcinoma: helical computed tomography findings in 30 patients. *J Comput Assist Tomogr* 2003; 27: 117–124.
23. Singh S, Chakraborty S, Bonthu N, et al. Combined hepatocellular cholangiocarcinoma: A case report and review of literature. *Dig Dis Sci* 2013; 58: 2114–2123.
24. Bolondi L, Cillo U, Colombo M, et al. Position paper of the Italian Association for the Study of the Liver (AISF): The multidisciplinary clinical approach to hepatocellular carcinoma. *Dig Liver Dis* 2013; 45: 712–723.
25. Panjala C, Senecal DL, Bridges MD, et al. The diagnostic conundrum and liver transplantation outcome for combined hepatocellular-cholangiocarcinoma. *Am J Transplant* 2010; 10: 1263–1267.
26. Albrecht T, Blomley M, Bolondi L, et al. Guidelines for the use of contrast agents in ultrasound. *Ultraschall Med* 2004; 25: 249–256.
27. Lee JI and Campbell JS. Role of desmoplasia in cholangiocarcinoma and hepatocellular carcinoma. *J Hepatol* 2014; 61: 432–434.
28. Sirica AE and Gores GJ. Desmoplastic stroma and cholangiocarcinoma: Clinical implications and therapeutic targeting. *Hepatology* 2014; 59: 2397–2402.
29. D’Onofrio M, Vecchiato F, Cantisani V, et al. Intrahepatic peripheral cholangiocarcinoma (IPCC): Comparison between perfusion ultrasound and CT imaging. *Radiol Med* 2008; 113: 76–86.
30. Wilson SR, Kim TK, Jang HJ, et al. Enhancement patterns of focal liver masses: Discordance between contrast-enhanced sonography and contrast-enhanced CT and MRI. *AJR Am J Roentgenol* 2007; 189: W7–W12.
31. Piscaglia F, Salvatore V and Borghi A. Contrast enhanced imaging pattern of central scar in focal nodular hyperplasia. *Ultrasound Med Biol* 2010; 36: 2146–2147.
32. Loyer EM, Chin H, DuBrow RA, et al. Hepatocellular carcinoma and intrahepatic peripheral cholangiocarcinoma: Enhancement patterns with quadruple phase helical CT – a comparative study. *Radiology* 1999; 212: 866–875.
33. Gaiani S, Celli N, Piscaglia F, et al. Usefulness of contrast-enhanced perfusional sonography in the assessment of hepatocellular carcinoma hypervascular at spiral computed tomography. *J Hepatol* 2004; 41: 421–426.